AFRL-SN-WP-TP-2006-123

THE CALIBRATION OF FOUR-ARM SPIRAL MODAL MEASUREMENTS FOR ANGLE-OF-ARRIVAL DETERMINATION (PREPRINT)

Joshua S. Radcliffe, Krishna M. Pasala, and Stephen W. Schneider

JULY 2006

Approved for public release; distribution is unlimited.

STINFO COPY

SENSORS DIRECTORATE
AIR FORCE RESEARCH LABORATORY
AIR FORCE MATERIEL COMMAND
WRIGHT-PATTERSON AIR FORCE BASE, OH 45433-7320

REPORT DOCUMENTATION PAGE

Form Approved
OMB No. 0704-0188

1. REPORT DATE *(DD-MM-YY)*	2. REPORT TYPE	3. DATES COVERED *(From - To)*
July 2006	Conference Paper Preprint	05/01/2004 – 05/01/2006

4. TITLE AND SUBTITLE
THE CALIBRATION OF FOUR-ARM SPIRAL MODAL MEASUREMENTS FOR ANGLE-OF-ARRIVAL DETERMINATION (PREPRINT)

5a. CONTRACT NUMBER
In-house

5b. GRANT NUMBER

5c. PROGRAM ELEMENT NUMBER
N/A

6. AUTHOR(S)
Joshua S. Radcliffe and Stephen W. Schneider (AFRL/SNDR)
Krishna M. Pasala (University of Dayton)

5d. PROJECT NUMBER
7622

5e. TASK NUMBER
11

5f. WORK UNIT NUMBER
0D

7. PERFORMING ORGANIZATION NAME(S) AND ADDRESS(ES)
RF and EO Subsystems Branch (AFRL/SNDR)
Aerospace Components & Subsystems Technology Division
Sensors Directorate
Air Force Research Laboratory, Air Force Materiel Command
Wright-Patterson Air Force Base, OH 45433-7320

University of Dayton
300 College Park
Dayton, OH 45469

8. PERFORMING ORGANIZATION REPORT NUMBER
AFRL-SN-WP-TP-2006-123

9. SPONSORING/MONITORING AGENCY NAME(S) AND ADDRESS(ES)
Sensors Directorate
Air Force Research Laboratory
Air Force Materiel Command
Wright-Patterson Air Force Base, OH 45433-7320

10. SPONSORING/MONITORING AGENCY ACRONYM(S)
AFRL-SN-WP

11. SPONSORING/MONITORING AGENCY REPORT NUMBER(S)
AFRL-SN-WP-TP-2006-123

12. DISTRIBUTION/AVAILABILITY STATEMENT
Approved for public release; distribution is unlimited.

13. SUPPLEMENTARY NOTES
PAO Case Number: AFRL/WS 05-2059, 06 Sep 2005. This work has been submitted for publication in the Proceedings of the 2005 Annual Symposium of the Antenna Measurement Techniques Association (AMTP 2005). One or more of the authors is a U.S. Government employee working within the scope of their Government job; therefore, the U.S. Government is joint owner of the work. If published, AMTP may assert copyright. The Government has the right to copy, distribute, and use the work. All other rights are reserved by the copyright owner.

14. ABSTRACT
Direction Finding (DF) systems have long been an area of intense research within the Air Force Research Laboratory. There are presently two types of existing DF systems: wideband multi-mode antennas and interferometers. Wideband multi-mode DF systems allow for a large bandwidth but present a low resolution and high variance. Interferometers provide high accuracy and low variance but are narrow band and require a large number of single aperture antenna elements. An effort has commenced to incorporate a broadband DF system with high resolution using two multi-mode spiral antennas. Using an interferometer of multi-mode elements, we can provide high resolution and wideband operation without using numerous antennas. This paper presents the results of extensive wideband measurements carried out on a four-arm spiral antenna and the associated modeformer. These measurements are used to assess and validate the angle estimation capability of the multi-arm spiral antenna.

15. SUBJECT TERMS
Interferometer, Direction Finding, Angle of Arrival, spiral antennas, multi-mode antennas

16. SECURITY CLASSIFICATION OF:			17. LIMITATION OF ABSTRACT:	18. NUMBER OF PAGES	19a. NAME OF RESPONSIBLE PERSON (Monitor)
a. REPORT	b. ABSTRACT	c. THIS PAGE			Joshua Radcliffe
Unclassified	Unclassified	Unclassified	SAR	14	19b. TELEPHONE NUMBER *(Include Area Code)* N/A

Standard Form 298 (Rev. 8-98)
Prescribed by ANSI Std. Z39-18

The Calibration of Four-arm Spiral Modal Measurements for Angle-of-Arrival Determination

Joshua S. Radcliffe
Air Force Research Laboratory, AFRL/SNRR
2241 Avionics Circle, Bldg 620
Wright Patterson AFB, Ohio 45433
joshua.radcliffe@wpafb.af.mil

Krishna M. Pasala
University of Dayton
300 College Park
Dayton, OH 45469
krishna.pasala@notes.udayton.edu

Stephen W. Schneider
Air Force Research Laboratory, AFRL/SNRR
2241 Avionics Circle, Bldg 620
Wright Patterson AFB, Ohio 45433
Stephen.schneider@wpafb.af.mil

ABSTRACT

Direction Finding (DF) systems have long been an area of intense research within the Air Force Research Laboratory. There are presently two types of existing DF systems: wideband multi-mode antennas and interferometers. Wideband multi-mode DF systems allow for a large bandwidth but present a low resolution and high variance. Interferometers provide high accuracy and low variance but are narrow band and require a large number of single aperture antenna elements. An effort has commenced to incorporate a broadband DF system with high resolution using two multi-mode spiral antennas. Using an interferometer of multi-mode elements, we can provide high resolution and wideband operation without using numerous antennas. This paper presents the results of extensive wideband measurements carried out on a four-arm spiral antenna and the associated modeformer. These measurements are used to assess and validate the angle estimation capability of the multi-arm spiral antenna.

Keywords: Interferometer, Direction Finding, Angle of Arrival, spiral antennas, multi-mode antennas.

1.0 Introduction

In recent years, a variety of approaches have been investigated to estimate the angle-of-arrival (AoA) of a distant emitter source. A few of these methods include interferometry [1], beam-forming techniques [2], and parameter estimation via signal processing techniques [3-4]. Multiple antenna elements are required for each of these methods; therefore, issues of maintainability, bandwidth, cost, size, weight, and power are constant drawbacks to these direction finding techniques. Realizing this, a new solution to this problem is desirable that will enhance the performance and eliminate the impediments present in current DF techniques. A single aperture multimode antenna is an attractive solution for use in deriving AoA estimates over a wide bandwidth [5]. More specifically, a multi-arm spiral antenna provides an attractive alternative to this problem. A multi-arm (and thereby multi-mode) spiral antenna possesses frequency independent characteristics including constant pattern, impedance, polarization, and phase center over a wide band of frequencies [6]. These frequency independent characteristics bolster the feasibility of spiral antennas as an attractive solution in deriving AoA estimates. Utilizing these antennas consists of combining the terminal outputs of the multiple arms into a Butler matrix "modeformer" and then deriving angle information from the outputs of the modeformer. Comparison of the phases of the modeformer outputs produces an estimate of the azimuth of an incoming signal, while the comparison of the magnitudes of the modeformer outputs gives an estimate of the elevation angle of an incoming signal. Figure 1 shows the geometry of a spiral and an incoming signal where φ is azimuth and θ is elevation.

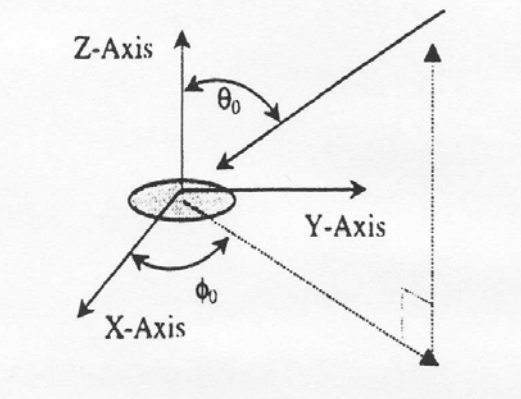

Figure 1: Incoming signal geometry of an N-arm spiral.

This "comparison" approach, as it is aptly named, when used with a 4-arm spiral antenna in conjunction with modeformer hardware provides AoA estimates whose accuracy is comparable to that of two single-mode antennas separated by one-half wavelength (a half-wave interferometer), over the entire bandwidth.

The work presented in this paper is the commencement of an effort to validate, by actual measurements, the performance of multi-mode four-arm spiral antennas in relationship to DF.

2.0 Existing DF Techniques

Interferometry is the most prevalent of existing DF techniques. The interferometer is a high-accuracy system which determines the emitter location by measuring the AoA along multiple baselines. A baseline is composed of two identical antennas one-half wavelength apart (the half-wave interferometer), two identical receivers, and a phase comparator. An interferometer system must contain at least two baselines to obtain both azimuth and elevation data, and is arranged in an L-shaped configuration. One more antenna must be added in each baseline at an electrically long length in order to obtain a more accurate estimate, while the electrically short baseline exists to resolve the ambiguity from the long baseline pair. This five-element system is known as the Linear Phase Interferometer (LPI). The LPI works well when the long baseline is long enough to provide the required accuracy and the short baseline is electrically short enough to remain unambiguous [7]. A significant problem with the interferometer method is that each of these baselines is narrowband. It takes numerous LPI's to add bandwidth to the entire system! A full interferometer system can easily contain up to three LPI's which is fifteen antennas—an entire "antenna farm." Figure 2 shows the typical setup of a full interferometer DF system used to determine AoA over a wide band of frequencies.

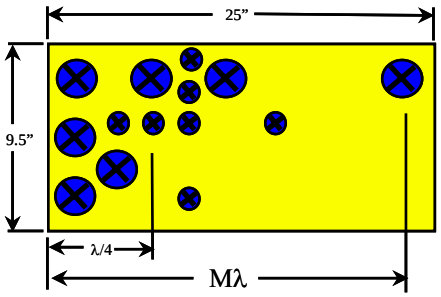

Figure 2: Typical interferometer "antenna farm."

The prominent catalyst in using a 4-arm spiral instead of a half-wave interferometer is the bandwidth of the AoA estimates; for a 4-arm spiral, these estimates remain constant over the entire band of frequencies for which the spiral antenna is devised.

3.0 Four-arm Spiral Measurements

As stated in the introduction of this work, the objective of this effort is to demonstrate the proposed theory with measured data. All measurements for this effort were performed in the Sensors Directorate's Radiation and Scattering Compact Antenna Laboratory (RASCAL). RASCAL is a compact far-field range used for smaller sized antenna aperture pattern and radar cross section measurements. In order to obtain accurate data from each spiral antenna, a phase-stationary test body was used in all 4-arm spiral measurements. When considering an antenna in the presence of a conducting surface, one must make a careful evaluation of the performance of that antenna in an appropriate environment. An antenna test body is required to close the distance between a conformal antenna host surface and the designer's infinite ground plane model. The "almond" shaped test body owned by RASCAL and used for all 4-arm spiral measurements in this project is a documented, proven, and patented device for high performance antenna measurements [8]. This "almond" test body incorporates a unique positioning system which provides a phase-stationary antenna aperture center under rotation of both azimuth and elevation. The result is that all 4-arm spiral measurements can be performed with the center of the spiral in a fixed position in the antenna test range incorporated in a test body of high performance with ground plane characteristics. Figure 3 and 4 show the diagram for the almond test body and the actual test body in RASCAL, respectfully.

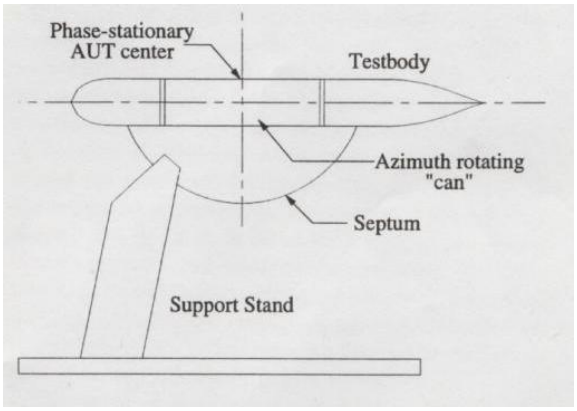

Figure 3: Phase-stationary test body diagram.

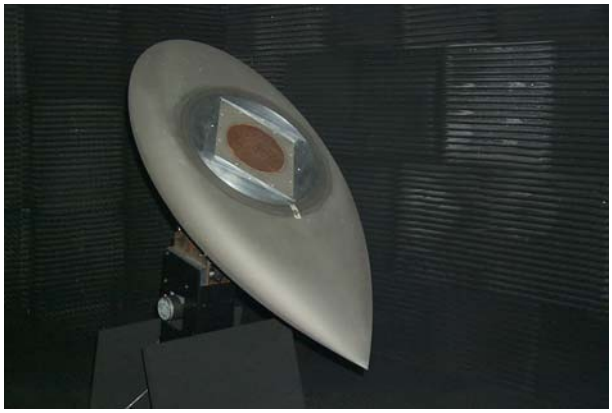

Figure 4: Actual test body in RASCAL compact range.

Azimuth patterns and phase of a four-arm spiral antenna were measured at three different elevation angles (θ =20°, 40°, and 45°). These angles were chosen per theory [9] of the modal pattern behavior of a four-arm spiral antenna and elevation measurements taken in RASCAL. Figures 5 presents elevation measurements of each usable mode that validate the elevation cut modal patterns of theory. It should be noted that the x-axis scale ranges from 0^o to 180^o rather than -90^o to 90^o in figure 5; boresight (the z-axis, see figure 1) in this plot is defined as the elevation angle of 90^o which is typically defined as 0^o. Elevation angles in this text described as 20^o, 40^o, or 45^o should be inferred to mean 90^o +/- 20^o, 40^o, or 45^o in figures hereafter.

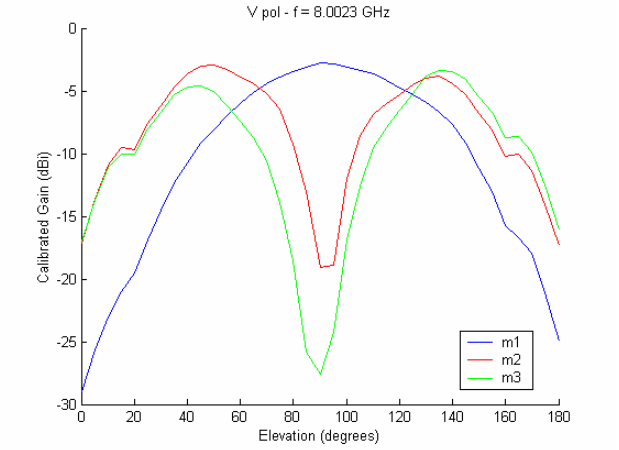

Figure 5: Measured elevation patterns at 8GHz.

Figures 6-14 illustrate the measured azimuth magnitude and phase data at 4GHz for each mode of a four-arm spiral antenna at elevation angles of θ= 20°, 40°, and 45°, respectively. All data shown corresponds to the case of vertical polarization for all three usable modes; azimuth is measured for φ = 0°- 360°. The purpose of this graph setup is to show the change in output as the mode number changes and to demonstrate the element to element differences. Note that theory [9] calls for the amplitude of the modal outputs to be constant with azimuth; however, in practice this is only approximately true as seen specifically throughout the actual measured data shown in the figures below. It is also of interest to note the difference in gain levels of the three modes at the different elevation angles. As per theory, the phases of the modal outputs vary linearly with azimuth and the slopes are directly related to the corresponding modal numbers. As may be seen from the experimental data, these relationships do hold, though the linearity is not perfect. These imperfections will lead to errors in the angle estimation.

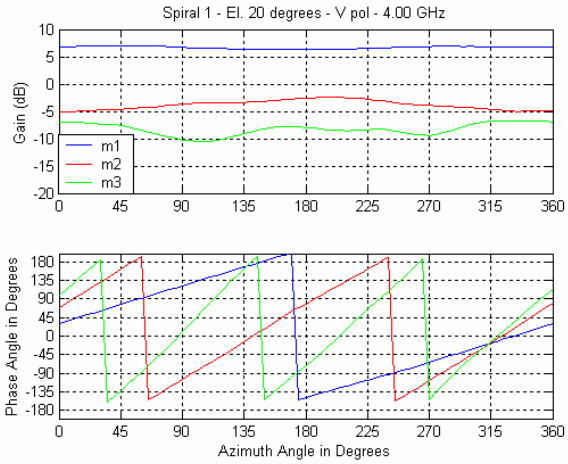

Figure 6: Measured azimuth magnitude and phase for θ =20° at 4GHz.

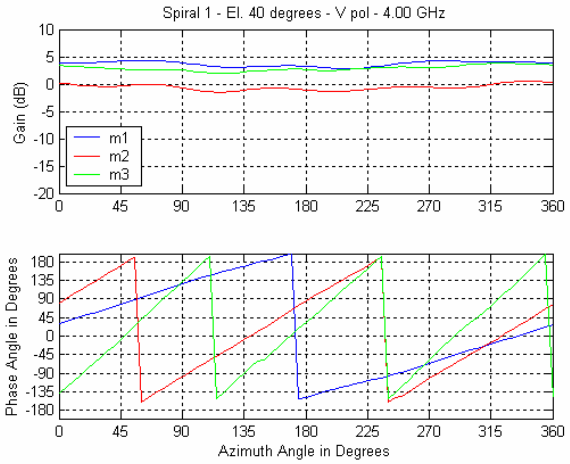

Figure 7: Measured azimuth magnitude and phase for θ =40° at 4GHz.

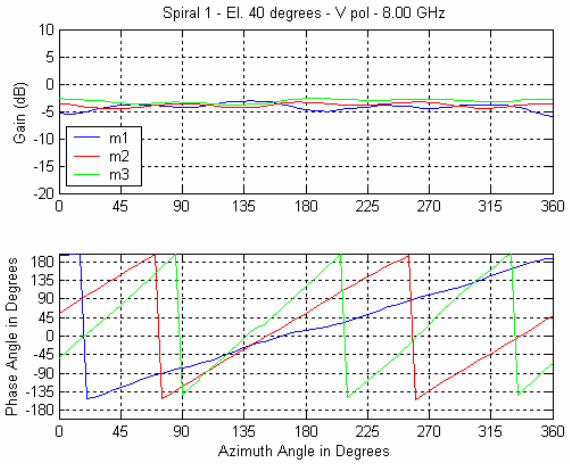

Figure 10: Measured azimuth magnitude and phase for θ =40° at 8GHz.

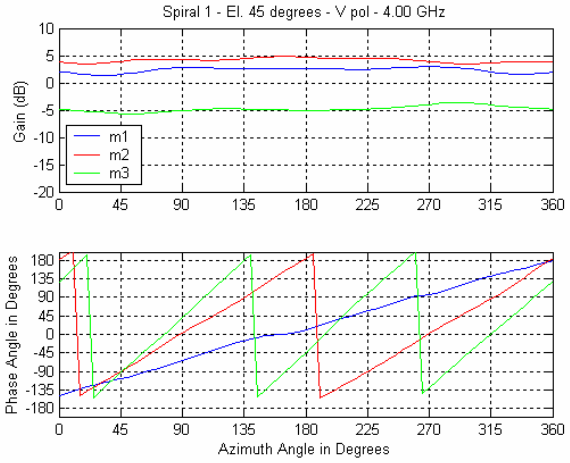

Figure 8: Measured azimuth magnitude and phase for θ =45° at 4GHz.

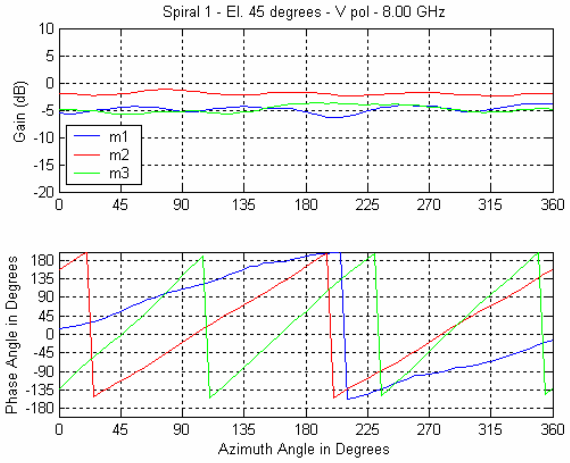

Figure 11: Measured azimuth magnitude and phase for θ =45° at 8GHz.

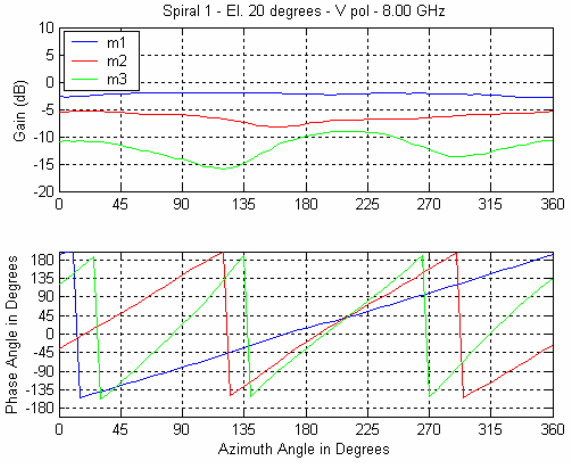

Figure 9: Measured azimuth magnitude and phase for θ =20° at 8GHz.

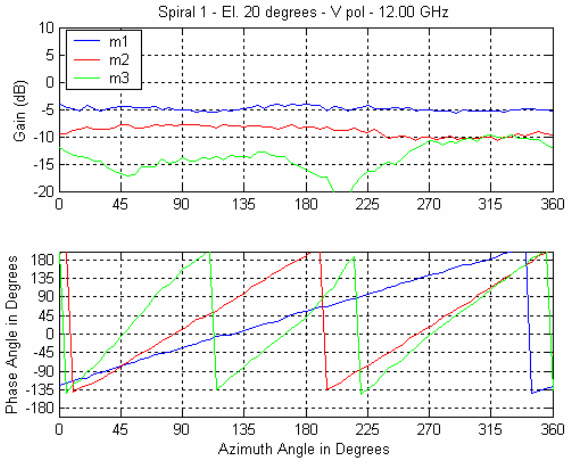

Figure 12: Measured azimuth magnitude and phase for θ =20° at 12GHz.

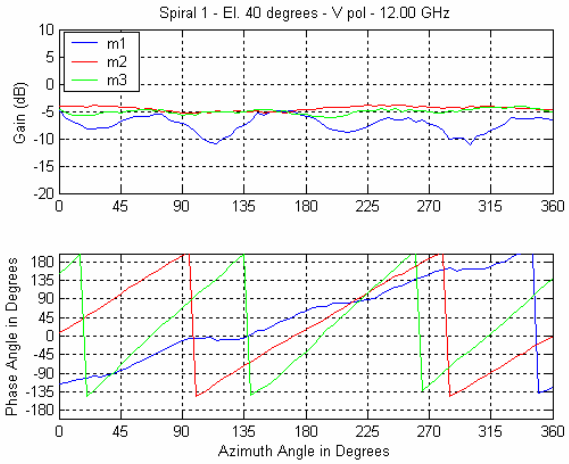

Figure 13: Measured azimuth magnitude and phase for θ =40° at 12GHz.

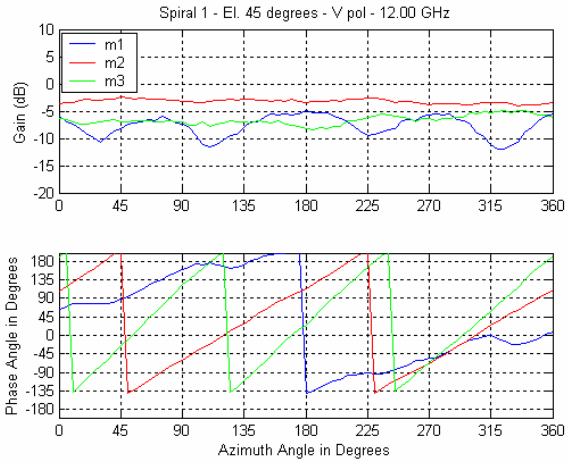

Figure 14: Measured azimuth magnitude and phase for θ =45° at 12GHz.

From an analysis of the data shown in figures 6-14, one can forge the following observations:

- The magnitudes of the modal outputs are relatively invariant with respect to azimuth, as predicted by theory.
- The phase angles of the modal outputs change linearly with azimuth as predicted by theory. Indeed, this is the crucial result that makes possible the determination of azimuth from the modal output measurements. It may be noted, however, that the linearity is not perfect and leads to errors in azimuth angle estimation.
- The slope of the phase vs. azimuth angle increases linearly with the mode number, again precisely as predicted by theory.
- The data clearly shows the differences in modal phase starting points for each mode at φ = 0°; this observation demonstrates the need and importance of calibration. The incident field at the phase reference (especially the phase) is different for each measurement and must be properly accounted for to obtain reliable AoA measurements.

Figures 12-14 show the azimuth data at 12GHz and exemplify the experimental data in the upper portion of the 8-12GHz band. The observations made above continue to be valid except for a more pronounced appearance of ripple. This "ripple" is observed in particular at the high end of the band and may be due to the active region approaching the feed region. Any small asymmetries or imperfections in the feed are likely to affect the active region, especially for mode 1, at higher frequencies. It is reasonable to expect this increased "ripple" to manifest as increased variance in the azimuth angle estimates at the higher end of the band.

4.0 Calibration

The calibration of the collected phase data, as mentioned in the previous section, is a necessity as part of the process of determining AoA for a four-arm spiral antenna. As mentioned in the introduction, the phase comparison of the modeformer output of a spiral is how azimuth is estimated. The differences in the phase offset at φ = 0° in figures 6-14 demonstrate the need for calibration. Only by knowing the actual position of each linear modal phase progression can one obtain an accurate estimate of azimuth. For each azimuth phase measurement, a calibration is required to align each linear modal phase plot; a phase value of 0° is aligned at φ = 0° for each azimuth measurement. Figure 15 shows calibrated phase data for one measurement case.

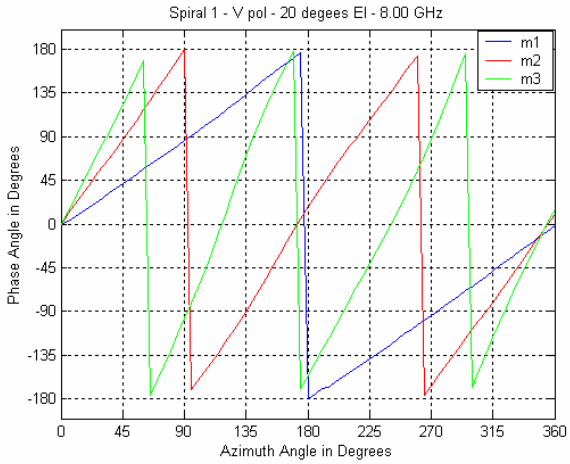

Figure 15: Calibrated phase data for θ =20° at 8GHz.

After calibration, one can clearly observe the new common reference point (starting point) for the phase and

more clearly observe the unique slopes respective to each mode that increase as the mode number increases.

As aforementioned, it is these unique linear phase progressions that allow azimuth angle estimation using the "comparison" approach described in the introduction. An incoming signal is received by the spiral antenna at a specific elevation angle and a specific azimuth angle. The accuracy of an angle estimate is dependent on the amount of spatial coverage the antenna exhibits; this is demonstrated by the antenna pattern of the spiral. As observed in the azimuth measurements of figures 6-14, the four-arm spiral antenna magnitude stays relatively constant over 360° azimuth coverage but elevation pattern coverage, as noted in figure 5, varies by mode. Where the gain is low, corresponding angle estimates are not as accurate. For example, an incoming signal at an elevation angle on the horizon will not obtain very good spatial coverage from any mode, while an incoming signal at an elevation angle of boresight will only obtain spatial coverage from mode 1. Thus, the elevation angle of an incoming signal will determine which mode may provide the most accurate azimuth estimate (Note: only three elevation angles are available in measured data within this paper: θ =20°, 40°, and 45°).

Azimuth is estimated by comparing the modeformer phase outputs of the spiral antenna. The compensated phase of mode 1 may be used to provide a coarse estimate of the azimuth AoA. Recognizing that higher rates of phase change, or steeper slopes of phase, with respect to azimuth produce better accuracy of the estimate, a more accurate estimate may be obtained by using the phase corresponding to a higher mode. However, azimuth estimation using a higher order mode is ambiguous. For example, mode *n* provides *n* number of azimuth estimates over of 360° of azimuth. This ambiguity may be resolved using the coarse estimate provided by mode 1 [5].

Using this described process and the actual calibrated phase data from the phase measurements performed, it is possible to conduct an experiment to test the accuracy and validity of this AoA determination technique.

5.0 Experimentation

In order to test the accuracy and validity of the comparison technique of AoA determination, multiple Monte Carlo experiments were conducted using the actual azimuth measurement data collected in the RASCAL compact range. Signal-to-noise ratio (SNR), frequency, and elevation angle are the three independent variables considered for these experiments. One variable is varied while all others are kept constant in order to analyze the effects of each on the model. Noise is synthetically added to the experimental data, which is considered to be "pristine." For each experiment, statistics are recorded including mean, standard deviation, bias, and the number of catastrophic failures. Catastrophic failures are defined as AoA estimates that are greater than 7.5° away from the true AoA. When these catastrophic failures are identified, they are not included in the final statistical analysis for each measurement set.

The first experiment conducted varied SNR from 0 to 40 dB in 2.5 dB increments. Statistics were recorded at three elevation angles (θ =20°, 40°, and 45°) and at three frequencies (f=4, 8, and 12GHz), for each of the three usable modes. This Monte Carlo experiment generated 100 (N=100, the number of iterations) random azimuth angles from φ = 0°- 360° and the statistics were recorded from the obtained data. The following three figures show the effect of SNR on the number of catastrophic failures present in the azimuth estimates of the comparison method. As predicted in the previous section, when the elevation gain of the spiral is low for a particular elevation AoA, the number of catastrophic failures in the azimuth estimates skyrocket. Mode 1 in figure 18 is a perfect example of this trend. Also noticeable is the drastic decrease of the number of catastrophic failures as SNR increases for each elevation angle case; this alludes to the increase in accuracy for all estimates. Figures 16-18 are all cases at a frequency of 4GHz.

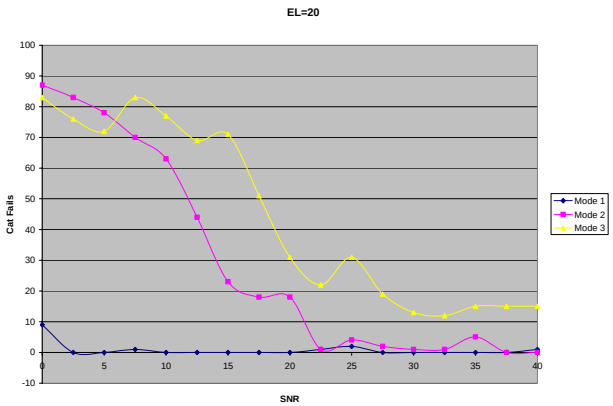

Figure 16: SNR vs. # of catastrophic failures for θ =20° at 4GHz.

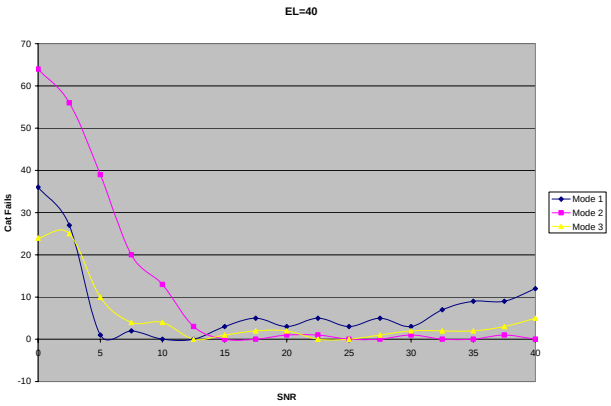

Figure 17: SNR vs. # of catastrophic failures for θ =40° at 4GHz.

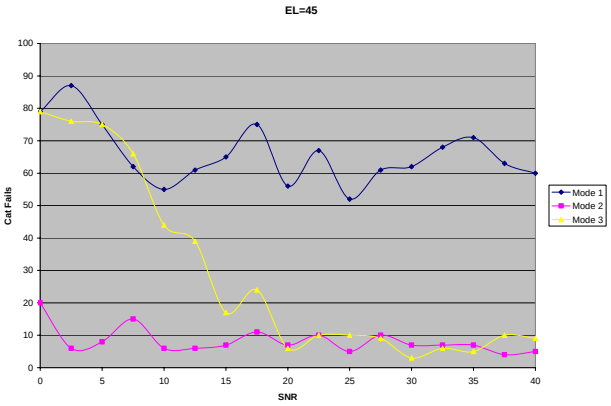

Figure 18: SNR vs. # of catastrophic failures for θ =45° at 4GHz.

The second experiment conducted varied frequency from 4-12GHz at three values: 4, 8, and 12GHz. SNR was kept constant at 20 dB. Monte Carlo experiment number two also generated 100 random azimuth angles from φ = 0°- 360° and the statistics were recorded from the obtained data. Cases were run for three elevation angles (θ =20°, 40°, and 45°) for each of the three usable modes. Results from this experiment were very simple relationships. As frequency increased, the number of catastrophic failures drastically increased for each case; this in turn raised the standard deviation for each case. This trend proves an observation made in the last sentence of section three: "it is reasonable to expect this increased "ripple" [present in the phase measurements of the upper frequency band] to manifest as increased variance in the azimuth angle estimates at the higher end of the band." However, the maximum standard deviation present in this experiment was only 4.5°.

The third and final Monte Carlo experiment generated 100 iterations of each of eight azimuth angles, two per each quadrant of coverage, which were chosen randomly ahead of time. These angles were φ = 30°, 60°, 135°, 150°, 200°, 225°, 300°, and 330°. 100 iterations were taken of each of these values for the three elevation angles (θ =20°, 40°, and 45°), three frequencies (4, 8, and 12GHz), and SNR=20 dB for each of the three usable modes. The statistics were recorded from the obtained data. The means of each of the three frequencies are shown in figures 19-21.

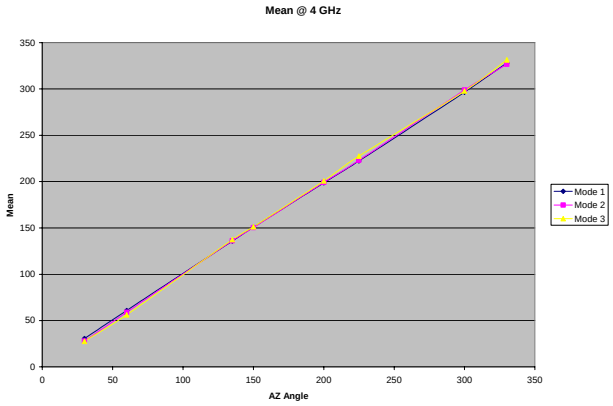

Figure 19: Mean of azimuth estimates for 4GHz.

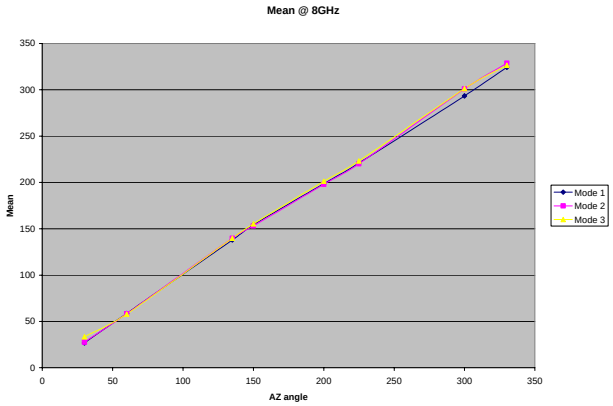

Figure 20: Mean of azimuth estimates for 8GHz.

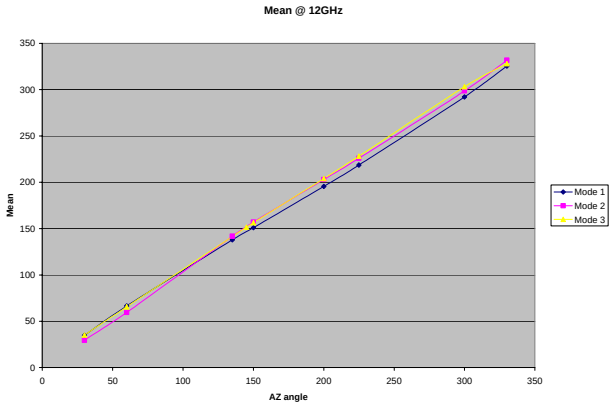

Figure 21: Mean of azimuth estimates for 12GHz.

The linearity and constant slopes of the above mean versus azimuth graphs indicate that the mean of the actual azimuth estimates is very close in value to the actual azimuth angles. This is in fact, true: the average

bias for mode 1, 2, and 3 in the above graphs are shown in table 1, below.

Figure			
Mode	19	20	21
1	1.5208°	3.686°	4.7504°
2	1.5169°	2.6105°	2.7289°
3	2.0618°	2.9026°	4.4703°

Table 1: Average bias of experiment 3 estimates.

Noticing the trends in table 1, one can observe that as frequency increases, the average bias of estimates increases. We can again relate this trend back to the final paragraph of section 3, as in the 2nd experiment. It may be beneficial to note that the average bias of estimates for this entire experiment is +/- 2.916°. It should also be mentioned that the number of catastrophic failures present in this experiment is drastically reduced from the previous experiments. The entire set of 4GHz estimates for this experiment contains zero catastrophic failures out of 2400 trials (24 angles of 100 iterations each)! The 8GHz set of estimates contains 187 failures out of 2400 trials. As expected, the 12GHz set of estimates contains the most catastrophic failures, 1005 out of 2400, or 41.8%.

6.0 Conclusions

A single 4-arm spiral antenna has been measured extensively in a high-performance phase-stationary test body in the RASCAL compact range. The magnitude and phase measurements have been processed, analyzed, and integrated into a robust algorithm to test the validity of AoA determination from direct measurements. The algorithm was then used to design and execute three experiments to test the accuracy of azimuth angle estimation using the comparison method [5]. The results show the broadband capabilities of the multi-mode spiral antenna for azimuth angle estimation. It has been demonstrated that azimuth estimation accuracy increases as SNR increases. It has been shown that the bias of the estimates tends to increase as frequency increases. This may be linked to the "ripple" in the phase measurements referred to at the end of section three.

Future work includes a statistical analysis of elevation angle estimates as well as verifying the performance of a novel dual spiral hybrid interferometer system [10].

7.0 References

1. Jacobs, E., and Ralston, E.W., "Ambiguity resolution in Interferometry", *IEEE Transactions on Aerospace and Electronic Systems*, AES-17, 6 (November 1981).
2. Johnson, D.H., and Dudgeon, D.E., *Array Signal Processing*, Englewood Cliffs, NJ: Prentice Hall, 1993.
3. Compton, R.T., "Adaptive Maximum Likelihood Angle Estimate Bias with a Monopulse Antenna under Ideal Conditions," Technical Report 95-5-4, WPAFB, OH, 1995.
4. Thierrien, C.W., *Discrete Random Signals and Statistical Signal Processing*, Englewood Cliffs, NJ: Prentice Hall, 1992.
5. Penno, R.P. and Pasala, K., "A Theory of Angle Estimation Using a Multi-arm Spiral Antenna", *IEEE Transactions on Aerospace and Electronics Systems*, 37, 1 (January 2001), 123-133.
6. Rumsey, V.H., *Frequency Independent Antennas*, Academic Press, New York & London: 1966.
7. Schneider, S.W., Penno, R.P., Pasala, K., and Kempel, L., "New Ways to Locate a Threat," Aircraft Survivability, Fall 2003, pp. 31-35.
8. Shamansky, H., Dominek, A., Schneider, S.W., Hughes, J., and Breaks, J., "A Phase-Stationary High Performance Antenna Test Body," *Antenna Measurement Techniques Association (AMTA) Annual Symposium proceedings*, 1995.
9. Corzine, R.G., and Mosko, J.A., *Four-Arm Spiral Antennas*, Norwood, MA: Artech House, 1990.
10. Pasala, K., Penno, R.P., Schneider, S., "Novel Wideband Multimode Hybrid Interferometer System," *IEEE Transactions on Aerospace and Electronics Systems*, 39, 4 (October 2003), 1396-1406.